Iraqi National Journal of Earth Science

www.earth.mosuljournals.com

Geomorphological Analysis of Chemical Weathering Features in Al-Band Hills Area, Eastern of Misan Governorate, Iraq

Bashar F. Maaroof [1] , Hashim H. Kareem [2]

[1,] *Babylon Center for Civilization and Historical Studies (B.C.C.H.S), University of Babylon, Hillah, Babil, Iraq.*

[2,] *Department of Geography, Faculty of Basic Education, University of Misan, Amarah, Misan, Iraq.*

Article information

Received: 17- Dec -2022

Revised: 06- Feb -2023

Accepted: 17- Mar -2023

Available online: 30- June- 2023

Keywords:
Geomorphological Features
Chemical Weathering
Soil Minerals
GIS

Correspondence:
Name: Bashar F. Maaroof

Email: basharma@uobabylon.edu.iq

ABSTRACT

A 59 km2 area of soil transect called Al-Band Hills in the eastern part of Misan governorate, south of Iraq was studied. The objective of this study was to understand the behavior of minerals and features of chemical weathering in the transect area soils that developed on fluvial and water-loaded sediments, to fulfill this objective, three soil pedons were selected one of them at the top of Hills and second in the middle and third Pedon in the bottom of the Hill. The results showed that Al-Band Hills located in semi-arid soils in the east of Misan governorate, south of Iraq are characterized by a low and middle intensity of chemical weathering. In an alkaline environment according to its carbonate minerals richness, with a low amount of precipitation, the intensity, and type of silicate minerals weathering is restricted not only by the climate but by the chemical conditions of the soil solution. According to this study's findings, the intensity of weathering of present soil pedons is mostly inherited from the parent rocks which is transferred by the action of water movement from northern areas from Turkey and Iran which belongs to the Quaternary. This study will give clear sights into the geomorphological and geochemical processes that happen in studied soils in semi-arid regions and show the possibility of using weathering features in carbonate and alkali sediments.

DOI: 10.33899/earth.2023.137382.1034,

التحليل الجيومورفولوجى لمظاهر التجوية الكيميائية فى منطقة تلال البند، شرقى محافظة ميسان، العراق

بشار فؤاد معروف[1]، **هاشم حنين كريم**[2]

[1] مركز بابل للدراسات الحضارية والتاريخية، جامعة بابل، بابل، العراق.

[2] قسم الجغرافيا،كلية التربية الأساسية، جامعة ميسان، العمارة، ميسان، العراق.

معلومات الارشفة

تاريخ الاستلام: 17- ديسمبر -2022

تاريخ المراجعة: 06- فبراير -2023

تاريخ القبـول: 17- مارس-2023

تاريخ النشر الالكتروني: 30- يونيو-2023

الكلمات المفتاحية:

المظاهر الجيومورفولوجية

التجوية الكيميائية

معادن التربة

نظم المعلومات الجغرافية (GIS)

المراسلة:

الاسم: بشار معروف

Email: basharma@uobabylon.edu.iq

الملخص

تمت دراسة مساحة 59 كم 2 من التربة المقطعية تسمى تلال البند فى الجزء الشرقى من محافظة ميسان جنوبى العراق. كان الاختلاف فى متوسط هطول الأمطار السنوى داخل المقطع 12 مم/سنة، وكان متوسط درجة الحرارة السنوية 38 درجة مئوية. وكان الهدف من هذه الدراسة هو فهم سلوك المعادن وخصائص التجوية الكيميائية فى تربة المنطقة المقطوعة التى نشأت على الرواسب النهرية والمحملة بالمياه، من أجل تحقيق هذا الهدف، تم اختيار ثلاثة بيدونات تربة، واحدة منها فى الجزء العلوى من التلال والثانية فى الوَسَط والثالثة فى أسفل التل. أظهرت النتائج أن تلال البند الواقعة فى تربة شبه قاحلة شرق محافظة ميسان جنوبى العراق تتميز بانخفاض متوسط كثافة التجوية الكيميائية. فى بيئة قلوية وفقًا لغناها بالمعادن الكربونية، مع انخفاض كَمِّيَّة الأمطار، فإن كثافة ونوع معادن السيليكات تكون مقيدة ليس فقط بالمناخ ولكن أيضًا بالظروف الكيميائية لمحلول التربة. وفقًا لنتائج هذه الدراسة، فإن شدة التجوية لبدون التربة الحالية موروثة فى الغالب من الصخور الأم التى تم نقلها بفعل حركة المياه من المناطق الشِّمالية من تركيا وإيران التى تنتمى إلى العصر الرباعى. ستلقى هذه الدراسة نظرة واضحة على العمليات الجيومورفولوجية والجيوكيميائية التى تحدث فى التربة المدروسة فى المناطق شبه القاحلة وتظهر إمكانية استخدام خصائص التجوية فى رواسب الكربونات والقلويات.

DOI: 10.33899/earth.2023.137382.1034,

Introduction

Geomorphological features consider a reflection or a result of actions of geological processes and factors, one of the most effective processes on the minerals and rocks is weathering, which can be defined as the group of activities by which elementary minerals are breakdown, and either vanish or are transformed into stable secondary minerals (Delvigne and Stoops, 1990). Weathering transforms parent rocks into soil regolith, which can be habituated by plants' roots and organisms and used by humans for agricultural uses (Nhu Sang et al., 2018). Awareness of weathering and formation of secondary new minerals is essential for (i) an appropriate comprehension of universal biogeochemical cycles, (ii) the average of soil genesis versus soil erosion, (iii) the chemistry of ground and surface waters, and (iv) the rate of buffering of acid materials from anthropic depletion (Faksness et al., 2020).

Weathering of primary minerals and formation of secondary minerals is the dominant soil-forming process in materials containing appreciable amounts of easily weatherable minerals (Dupré et al., 2003). Most rocks and sediments contain weatherable primary minerals (Puttonen et al., 2021). The chemical, mineralogical, and physical properties of soils formed on such parent materials are largely determined by the amount, nature, and distribution of the secondary minerals (Kalinin et al., 2021; Yousefifard et al., 2015).

Weathering intensity can be used to predict a range of soil properties (Wilford, 2012). Weathering includes the chemical and physical (mechanical) processes correlated with the breakdown or transformation of rocks and minerals as affected by climatic factors above and within the Earth's crust (Hartmann and Moosdorf, 2011). Weathering is a precondition for rocks to be eroded, and it is the reaction between weathering and erosional activities, that is essential in comprehending the nature and development of land topography (Brosens et al., 2021).

Soil is a main product of weathering and therefore soil genesis is correlated with weathering intensity and its outputs (Hartmann et al., 2014). Chemical weathering plays a key role in the effects of minerals' characteristics, this type of weathering is most active in a wet climate and conditions of high precipitation rate, but sometimes plays an important role in the transformation and breakdown of some minerals in arid and semi-arid conditions and this phenomenon becomes clear because the weakness of minerals, and it's less resistance to weathering although the low rate of rainfall and moisture especially with a high temperature in summer, weathering intensity highly control the percentage to which primary minerals are transformed to secondary constituents including clay minerals and sesquioxide (Yusoff et al., 2022). There are changes in the hydrological, geochemical, and geophysical characteristics of the soil, as weathering intensity increases. The quality and spatial distribution of the soil is highly influenced by parent rocks and weathering degree (Dzombak and Sheldon, 2022; Négrel et al., 2013). At similar parent rocks and climates, high weathering intensity is reflected in an alteration of the type and quantity of secondary minerals (Adamu et al., 2021). As weathering intensity raises, clays such as hydrous mica and 2:1 expansible mineral change to more resistant clays such as kandite (Delvigne and Stoops, 1990; Yousefifard et al., 2015). With excessive leaching, Fe and Si can be leached, leaving Al-rich gibbsite remains, and divergence in the intensity of weathering associated with climate, topography, geology, vegetation, and time all affect the allocation of water in the soil and the earth's crust (Prajith et al., 2021).

Although the correlation models have been based on fieldwork information from erosional zones, the estimation of weathering intensity likewise has the importance to supply perceptions into weathering and geomorphological processes towards sedimentological terrains (Ojo et al., 2021). Depending on the origin and geochemical properties of the soil source bedrocks, weathering index can reflect active or less active depositional systems and the level to which the mineral has been weathered (Baldermann et al., 2021; Millot and Négrel, 2013). Intensely weathered fan deposits can be differentiated from more active alluvial fans with geochemical compounds that resemble their parent rocks (Bickle et al., 2018). This research aims to shed light on the effect of chemical weathering of primary and secondary minerals on the geomorphological characteristics of the Al-Band hills area east of Misan Governorate by using integrated weathering indices.

Materials and Methods

1. Study Area:

Al-Band hills are located in the eastern parts of the Misan Governorate, southern Iraq, specifically in the southern parts of the Al-Jazira Eastern region (Maaroof, 2017). Al-Band Hills is a geological structure formed by the confluence of three river basins (Al-Sharhani, Al-Teeb, and Abu Ghraibat), and it is bounded on the north by the Al-Sharhani drainage basin, on the south and east by the Abu Ghraibat drainage basin, and on the west by the Al-Teeb drainage basin (Maaroof and Kareem, 2022). It lies between latitude (32°16′17.2″N - 32°23′5.1″N) and longitude (47°09′23″E - 47°17′38.1″E) (Figures 1 and 2).

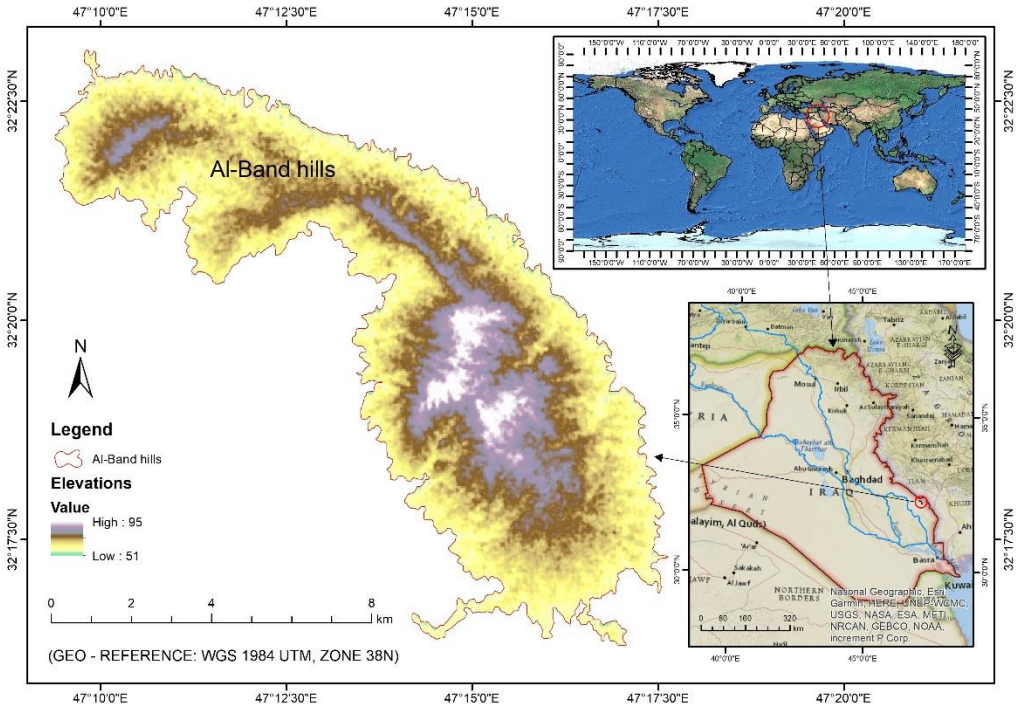

Fig. 1. The location of Al-Band Hills from Iraq.

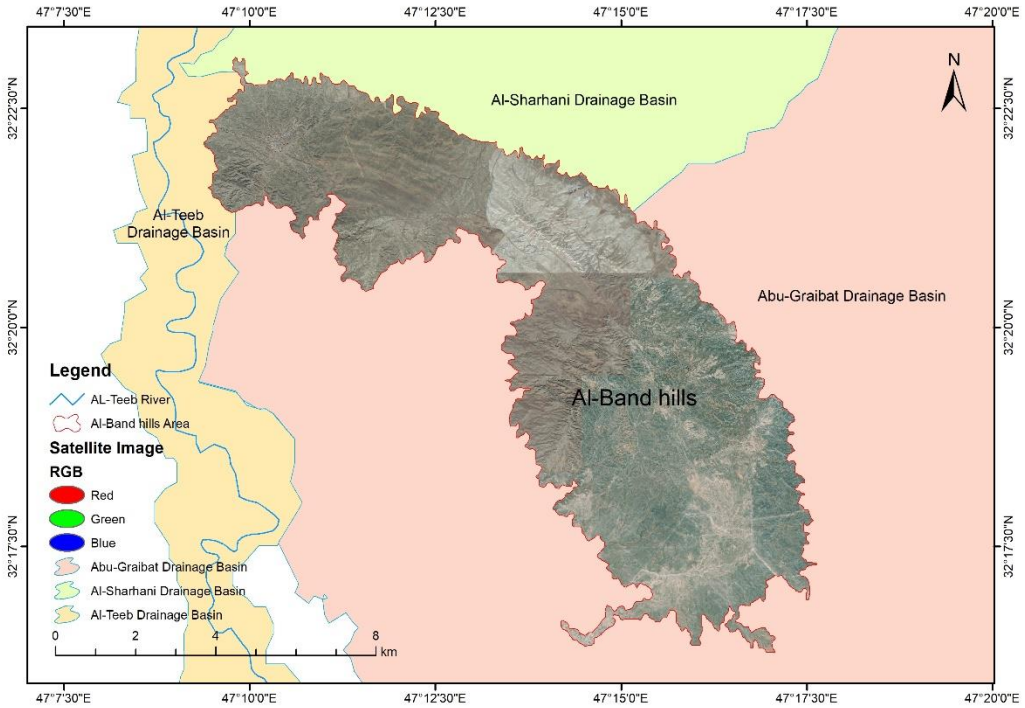

Fig. 2. Satellite image of Al-Band Hills.

The area of Al-Band Hills is 59 km2, with a perimeter of 80 km. The elevation levels varied in the area, as it consists of a complex topographic system that contains a set of landforms that earned it this characteristic. It has been classified into three terrain levels. The first region is between Contour Lines 90-70, the second region is between Contour Lines 69-60, and the third region is between Contour Lines 59-51, whereas, the highest elevation in the study area was 90 km (a.s.l), and the lowest was 51 (a.s.l) (Figures 3 and 4). There are many waterways in the study area, which are water channels formed by water erosion processes. After the end of the rain storm, the water collects and flows in areas with longitudinal extension and forms streams and then rivers, which in turn perform all geomorphological

processes (erosion and weathering) (Intisar Q. Hussein, 2014; Maitham A. Al-Ghanmi, 2015), (Figures 5). By examining the geological map of Iraq, it became clear that the study area is completely covered by the Bay Hassan Formation, which consists of a succession of sandstone and mudstone layers with intrusions of alluvial stone, and often contains sandstone layers and fine and medium-sized gravel, and that the sedimentation environment is fresh river water (Jassim S.Z. andGoffJ.C., 2006; Sissakian and Fouad, 2015).

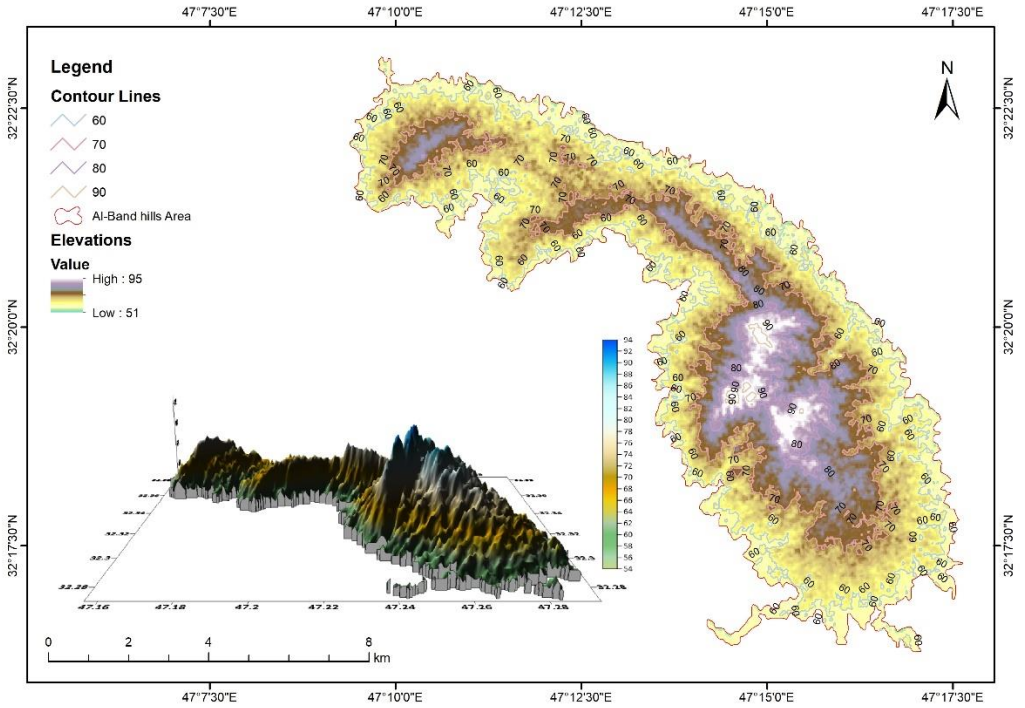

Fig. 3. Contour lines for Al-Band hills area.

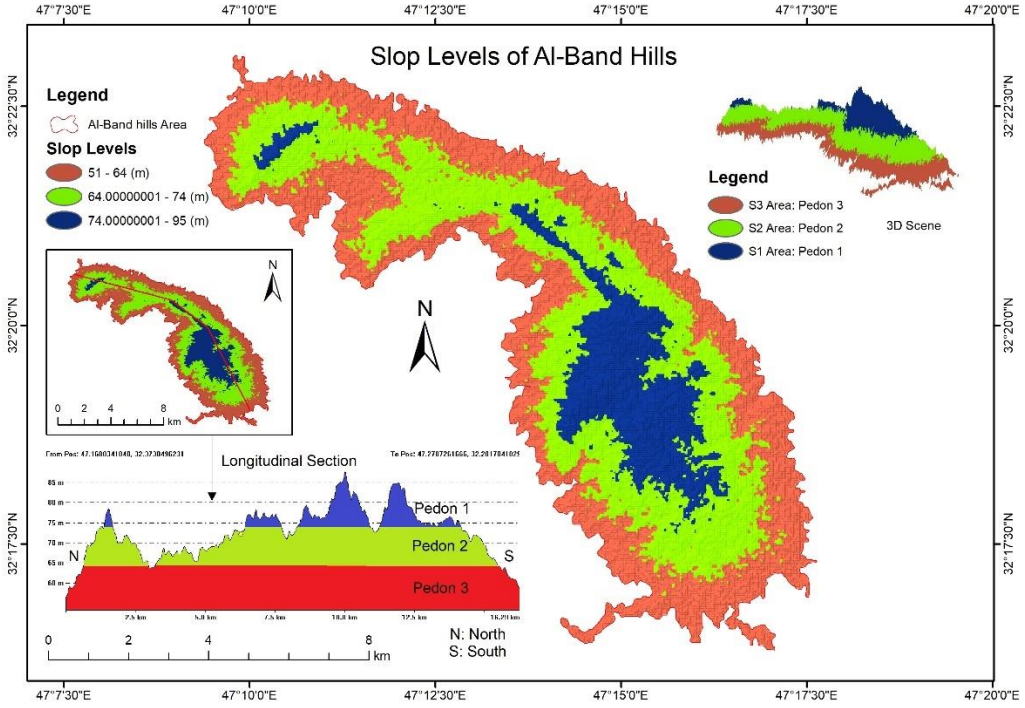

Fig. 4. Slope levels (%) for the Al-Band hills area.

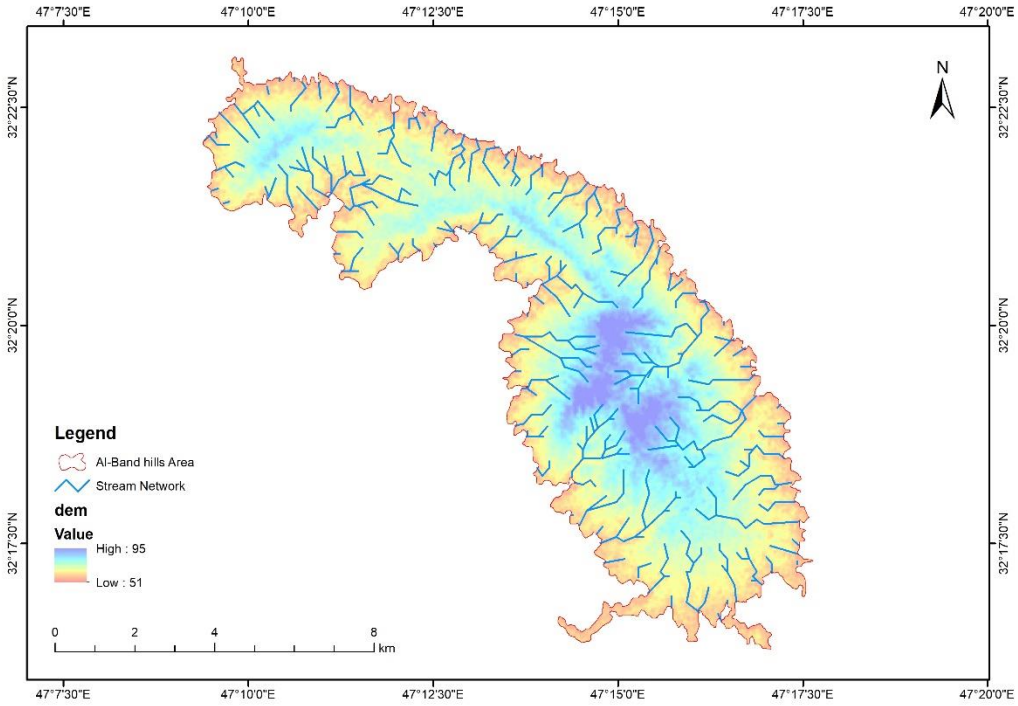

Fig. 5. The network of waterways in the Al-Band Hills area.

Climatically, the study area is characterized by the presence of two main seasons, namely the hot season of the year, which extends from the beginning of April until October (Maaroof, 2022a), and the cold season of the year, which extends from the beginning of November until the end of March approximately (Maaroof, 2022b). The summer season is characterized by heat and dryness, especially in the months (June, July, and August), as the temperature rates for these months are (37°C), (38.2°C) and (37.7°C), respectively, while the winter season is characterized by moderate temperatures with their tendency downward. The rainfall in the study area is characterized by its seasonality (Agha and Şarlak, 2016), as it falls on relatively distant periods, the duration of the precipitation is between October and May, and its annual average is (12) mm. (Table1).

Table 1. Climatic elements recorded in Al-Amarah Climatic Station for the period 1980-2009.

Months	temperature (°C)	Rainfall (mm)
January	16.2	34.5
February	19.5	22.6
March	24.2	31.7
April	30.9	13.3
May	40.7	2.1
June	45.7	-
July	47.2	-
August	45.2	-
September	42.1	-
October	35.2	5.7
November	25.7	14.5
December	20.1	19.7
Average and sum	32.7	144.1

2. Fieldwork:

To identify the weathering intensity and its reflectance on the geomorphological characteristics of the studied area the work had been done in two stages, the first stage identified the locations of the samples by dividing the study area into three transects, all transects including one soil Pedon was the locations selected in three different elevations, Pedon 1 in the upper part of Al-Band hills and Pedon 2 in the middle and Pedon 3 in the lower part of the hills, followed by prepare soil profiles to make morphological description according to soil survey staff (2021) and then determine boundaries of master horizons of

each profile. Soil samples were picked from each horizon with a weight of 1 kg and put in plastic bags for the second stage, which include laboratory analysis.

3. Lab. Analysis:

After bringing soil samples to the laboratory at the Faculty of Agriculture, University of Misan, the samples were air dried at room temperature, then ground with a wood hammer, sieved with a 2 mm sieve, and stored in a plastic container for analyses. Soil analyses include physical properties (soil texture, soil bulk density, particle density, and porosity) according to (Jacob H. Dane and G. Clarke Topp, 2002), chemical properties, soil reaction (PH), electrical conductivity Ec, cations, Anions, calcium carbonate, organic matter, and cation exchange capacity) according to (D. L. Sparks et al, 1996), and mineralogical composition (x-ray diffraction and scanning electron microscope SEM) according to (Ulery and Drees, 2008).

Results and Discussion

1. Soil Physical Properties:

The results in Tables 2 and 3 show the physical and chemical properties of studied soil Pedon's respectively, where the results can give us a clear picture of the soil behavior according to the physical and chemical weathering. The results in Table 2 showed that the percentages of soil fractions ranged between (200-340), (380-420) and (280-380) gm.kg-1 for clay, silt, and sand respectively, hence, this variation of soil fractions suggests the high percentage of clay and silt fractions which maybe occur as a result of sequential sedimentation by the cycle of wetting and drying and the transferring of soil particles between the parts of the hill. On the second hand the values of bulk ranged between (1.3-1.7) gm.cm-3 where a higher value was recorded in Pedon 2 subsurface horizon and a lower value recorded in Pedon 3 subsurface, this variation is highly correlated with the content of organic matter which effect of bulk density by making bridges between soil aggregates and improve the formation of good structure (Mills and Fey, n.d.; Saiz et al., 2012; Veras De Lima et al., 2013), while the results of particle density ranged between (2.64-2.72) gm.cm-3 were the highest value recorded in Pedon 3 at the surface horizon and the lowest value recorded in the same Pedon at the subsurface horizon, the results indicate that particle density in surface horizons is lower than subsurface horizons and this is due to the mineral composition in surface horizons is mixed with organic matter as well as the high porosity percentage compared with subsurface horizon (Ruehlmann, 2020). On the other hand, the value of porosity ranged between (38-48) % where the highest value is shown in Pedon 3 surface horizon while the lowest is recorded in Pedon 2 surface horizon, this range was correlated with the presence of clay where the clay fraction cause increasing in total specific area and porosity, and the distribution of clay was decreasing from the high Pedon which is Pedon 1 and increase in Pedon 3 in the bottom of the hill (Jackson, 2015).

Table 2. Some physical properties of studied soil pedons.

Pedon's	Horizon	Soil fractions gm.kg-1			Texture	Bulk density gm.cm^{-3}	Particle density gm.cm^{-3}	Porosity %
		Sand	Silt	Clay				
Pedon 1	surface	380	420	200	loam	1.4	2.65	47
	subsurface	340	390	270	Clay loam	1.6	2.70	41
Pedon 2	surface	320	400	280	Clay loam	1.5	2.66	38
	subsurface	300	400	300	Clay loam	1.7	2.72	44
Pedon3	surface	280	380	340	Clay loam	1.3	2.64	48
	subsurface	360	410	330	Clay loam	1.5	2.73	45

2. Soil Chemical Properties:

In order to shed light on chemical processes in the soil and to connect it with chemical weathering, some chemical analysis was done, the results in table 3 showed that the values of pH ranged between (7.2-7.8) where the highest value recorded in Pedon 3 in the subsurface horizon and the lowest value recorded in pedon2 surface horizon, this variation in soil PH is due to the difference in calcium carbonate percentage, while electrical conductivity EC ranged between (1.1-1.9) DS.m-1, and from this value, we can conclude that Pedon 3 was the higher in salinity while Pedon 1 was the lower one, and in general surface horizons record highest salinity compared with subsurface horizons and that because the action of leaching process which transfers the salts by mass flow from upper to lower positions in the hill, and because high temperature degrees which cause rising of groundwater by the capillary process to the surface then water evaporates leaving the salts on the surface as the white crust (Lybrand et al., 2011a).

Table 3. Some chemical properties of studied soil pedons.

Samples	horizon	pH	Ec Ds.m-1	organic matter gm.kg-1	CEC Cmol.kg-1	CaCO3 gm.kg-1
Pedon1	surface	7.4	1.2	15	20	320
	subsurface	7.7	1.1	12	23	347
Pedon2	surface	7.2	1.6	17	21	314
	subsurface	7.5	1.2	13	22	325
Pedon3	surface	7.4	1.9	22	25	319
	subsurface	7.8	1.7	15	24	337

The percentage of organic matter was low in general and ranged between (12-22) gm.kg-1(Table 3), and it gradually increases from upper locations to the lower Pedon. On the other hand, the surface horizon recorded a high quantity of organic matter as compared with the subsurface horizons (Table 3), this is due to the concentrations of plant roots and bioactivity in the surface layer (Herrero et al., 2003). Cation exchange capacity (CEC) ranged between (20-25) Cmol.kg-1 was the highest value recorded in the Pedon 3 surface horizon while the lowest value was recorded in the pedon1 surface horizon, the variation in CEC values is highly correlated with the percent of clay and organic matter and its dependence on the type and quantity of clay minerals and organic matter content as add to the pH values (Adamu et al., 2021). The quantity of calcium carbonate as shown in Table 3 is ranged between (314-347) gm.kg-1 where the higher value is recorded in the pedon1 subsurface while the lowest value recorded in the Pedon 2 surface horizon, all pedons are characterized by a high percentage of calcium carbonate which also indicate that the parent material of studied pedons is rich in carbonate minerals furthermore it's transferring from its original lime rocks by water flow (Mayer1’ and Mayer, n.d.).

The results in Table 4 showed that the concentration of cations ranged between (2.2-3.2), (1.3-1.8), (0.6-0.8), and (0.05-0.06) mmol kg-1 for soluble calcium, magnesium, sodium, and potassium respectively, and these results indicate that there is a variation of soluble cations in the soil pedons and calcium was the dominant cations according to the results of calcium carbonate which consider the main source of calcium in soil solution and soluble salts also contribute in the other cations and anions. On the other hand, soluble anions ranged between (3.1-3.6), (1.1-1.5), and (0.6-0.9) mmol kg-1 for bicarbonate, chloride, and sulfate respectively while carbonate ion was Nil (Table 4), this variation in the soluble anions reflects the state of soluble salts as the main source of anions (Voigt et al., 2020).

Table 4. Soluble cations and anions in studied soil pedons.

samples	horizon	Soluble cations mmol/kg				Soluble anions mmol/kg			
		Ca^{++}	Mg^{++}	Na^{+}	K^{+}	$HCO3^{-}$	$CO3^{=}$	Cl^{-}	$SO4^{=}$
Pedon1	surface	3.1	1.5	0.8	0.06	3.3	Nil	1.3	0.8
	subsurface	2.8	1.7	0.6	0.05	3.1	Nil	1.2	0.7
Pedon2	surface	2.2	1.3	0.7	0.06	3.4	Nil	1.4	0.9
	subsurface	2.7	1.4	0.7	0.05	3.2	Nil	1.1	0.8
Pedon3	surface	2.9	1.5	0.6	0.06	3.6	Nil	1.5	0.8
	subsurface	3.2	1.8	0.7	0.06	3.5	Nil	1.3	0.6

3. Soil Mineralogical Properties:

3.1. Mineral Composition of Coarse Fraction (Sand):

The mineral composition of the soil is a key factor in the process of evaluation of chemical weathering focusing on the percentage of low and high-weathering-resistant minerals gives a good hint on the state of weathering and its products (Graly et al., 2022), the results in table 5 showed that the minerals in sand fraction ranged between (14-20) %, (5-8) %, (4-7) %, (8-12), (43-50), (7-9) % and (5-10) % for quartz, feldspar, chlorite, illite, calcite, dolomite, and gypsum respectively. From these results, we can see that calcite was the most dominant mineral followed by quartz, and the origin of these minerals is from the parent rocks also some minerals are secondary minerals that formed from the weathering of primary minerals and minerals' transformation during the weathering process. On the other hand, the results indicate that quartz was a higher percentage in the upper Pedon 1 and gradually decreased in the bottom Pedon 3 which is appropriate with the percent of sand, also the existence of secondary minerals such as calcite, gypsum, chlorite, and illite in different levels is evidence of the activity of weathering and transformation of minerals (Lybrand et al., 2011b).

Table 5. Mineral composition of sand fraction for studied soil pedons

samples	horizon	quartz	feldspars	chlorite	illite	calcite	dolomite	gypsum
Pedon1	surface	20	5	5	8	50	7	5
	subsurface	17	8	4	10	45	9	7
Pedon2	surface	18	7	4	11	43	8	9
	subsurface	17	5	7	12	45	7	7
Pedon3	surface	14	5	7	11	49	7	8
	subsurface	16	5	4	12	45	8	10

3.2. Mineral Composition of Fine Fraction (Clay):

One of the most important soil components is clay fraction which is considered the finer part of soil fractions with an average diameter of less than 0.002 mm, and because of this size it possesses a higher specific surface area and according to that clay exhibits as a most active fraction with or without organic matter (Walk et al., 2022). The results in Table 6 showed the percentage of clay minerals in studied soil pedons which display that montmorillonite (from the smectite group) is the dominant clay mineral that belongs to 2:1 clay minerals (phyllosilicates) which ranged between (38-45)%, followed by mica ranged (23-32) % followed by chlorite (15-18)% followed by kaolinite (1:1) ranged (9-12)% followed by less mineral content Mica-Smectite mixed layer which ranged (2-7)%, these results support the assumption of the activity of chemical weathering in this area where the stages of weathering include the transformation of mica minerals to montmorillonite passing in the middle stage of weathering which is the formation of interstratified mixed layer minerals (Kalinin et al., 2021; Rozanov et al., 2017; Yousefifard et al., 2015). On the other hand, the distribution of clay minerals in the depth showed that the surface horizons have less clay content compared with the subsurface (Table 6), this may be to the transferring of clay fine particles by the

movement of water downward during the process of leaching which occurs during raining seasons (Kalinin et al., 2021).

Table 6. Mineral composition of clay fraction for studied soil pedons

Samples	horizon	Montmorillonite	Mica	Chlorite	Kaolinite	Mica-Smectite mixed layer
Pedon1	surface	40	23	15	10	7
	subsurface	45	24	19	11	6
Pedon2	surface	38	31	15	9	3
	subsurface	42	32	15	12	3
Pedon3	surface	38	25	17	9	5
	subsurface	41	27	18	12	2

3.3. Diagnosis of Weathering Features by Using a Polarized Optical Microscope:

The common minerals in the silt and sand are remains of the minerals in the original bedrock; hence, they are called primary minerals. The most dominant is the high resistance to weathering mineral quartz. Some minerals often associated, maybe in low amounts, are mica, feldspar, zircon, hematite, and limonite. If the soil is not strongly exposed to the leaching process, the sand and silt fractions may also contain pieces of dolomite and calcite (Favier et al., 2022)

Figure 6 shows that there is a set of minerals with different stages of weathering where light brown angular flaky Biotite is appearing covered with many holes of different sizes on the surfaces beside irregular alignment at the edges which indicates the effect of weathering (Fig. 6a), also altered biotite with the dark color associated with garnet and opaque iron oxide with black color (Fig. 6b). Figure 6c shows light green epidote with signs of weathering and figure 6d displays angular colorless prismatic zircon also appears with minimum signs of weathering, alkali feldspar also appears in a type of microcline, and it was highly affected by weathering process through many cracking and splitting's spreading on its surface (Fig. 6e).

Figure 7a shows an angular yellowish color staurolite mineral with clear angles and some holes on the surface as a result of weathering, also figure 7b shows altered brown flaky biotite with layer and edge weathering appearing beside fresh green chlorite which shows many holes on the surface with different sizes (Fig. 7c). Figure 7d shows rounded carbonate rock fragment which appears less effected by weathering, in image e prismatic very angular pyroxene also revealed with many weathering features such as holes and splitting and cracking in an elongated way (Fig. 7c).

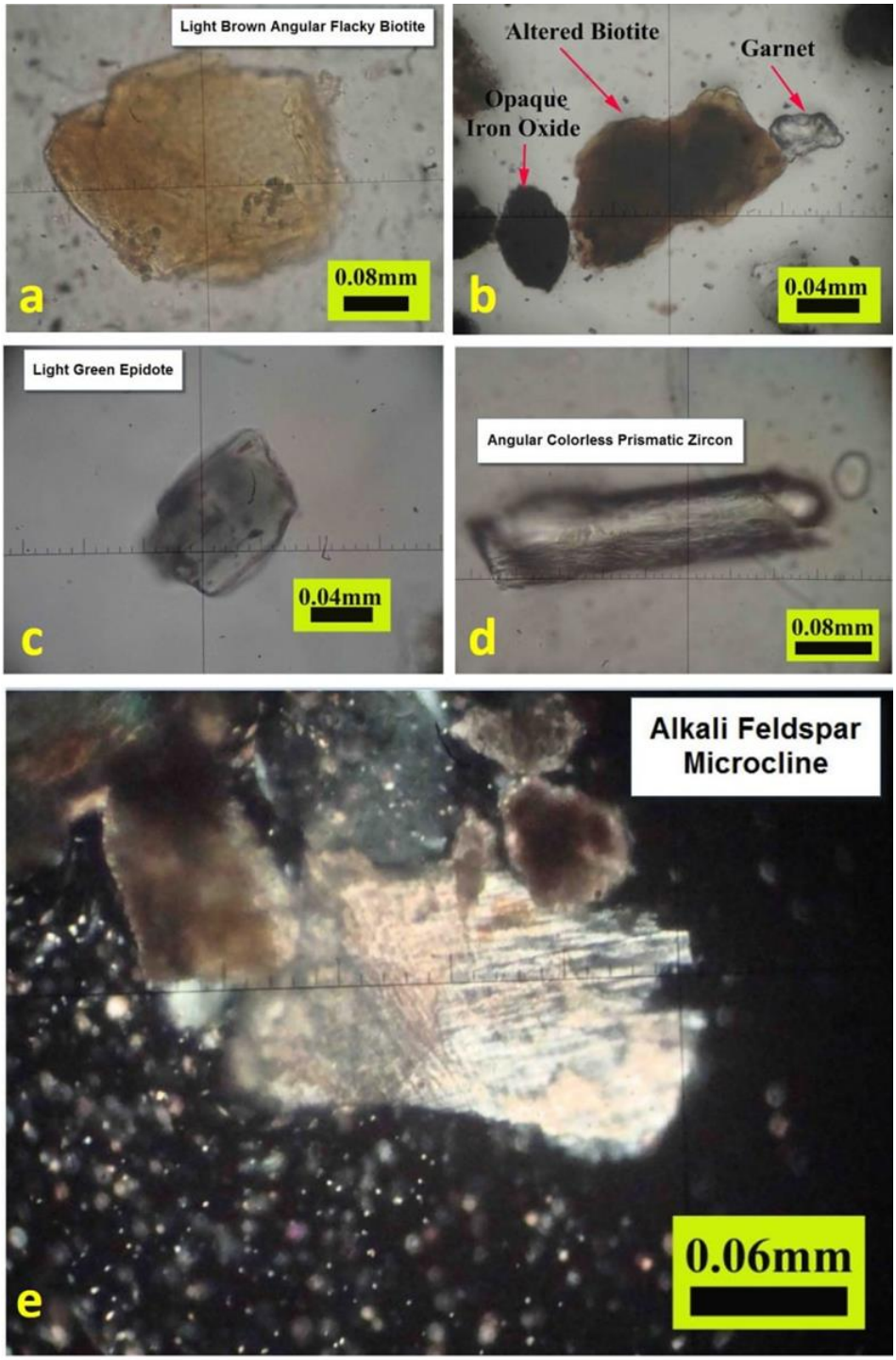

Fig. 6. Mineral composition of Pedon 1 surface and Pedon 2 subsurface horizon.

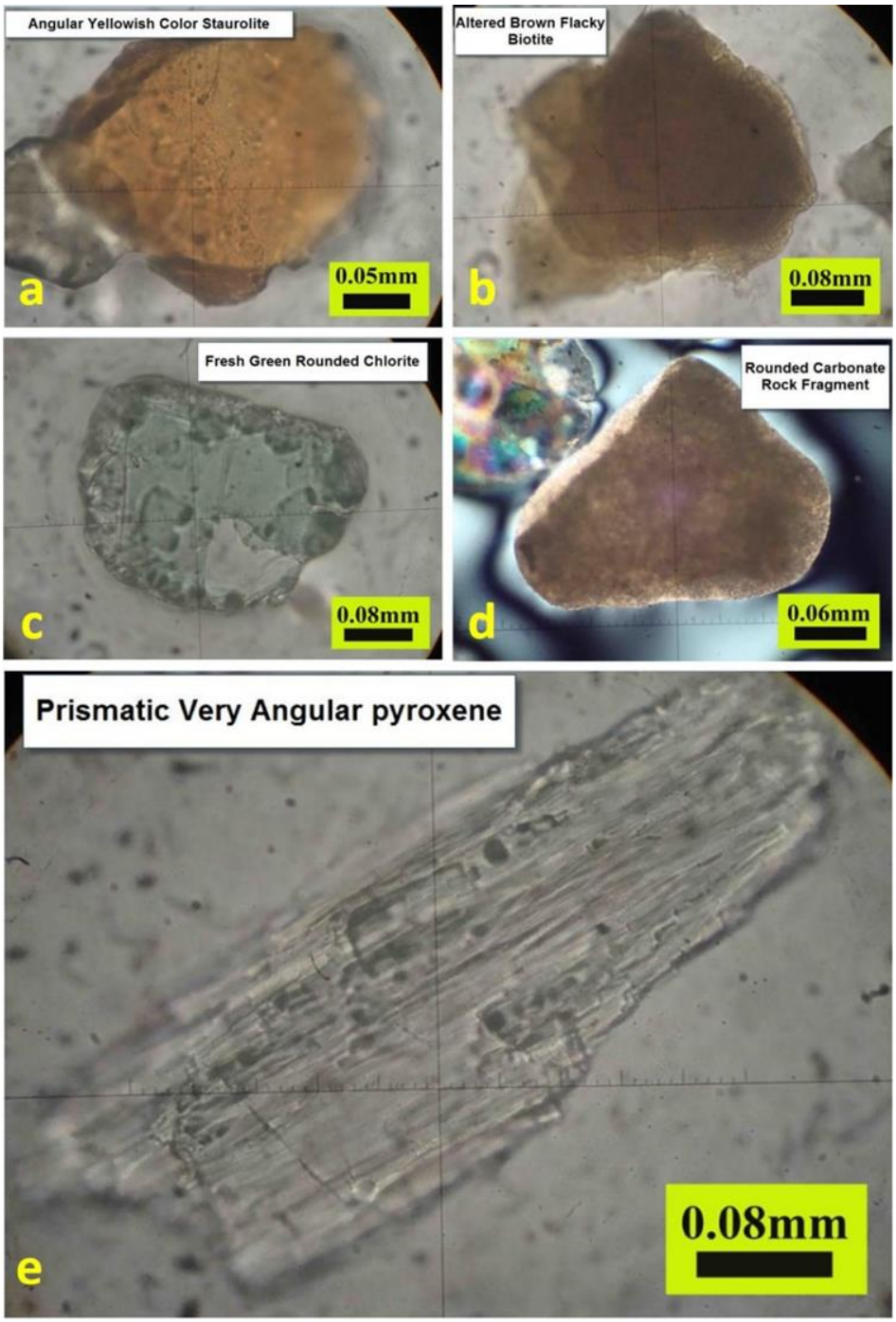

Fig. 7. Mineral composition of Pedon 2 surface horizon.

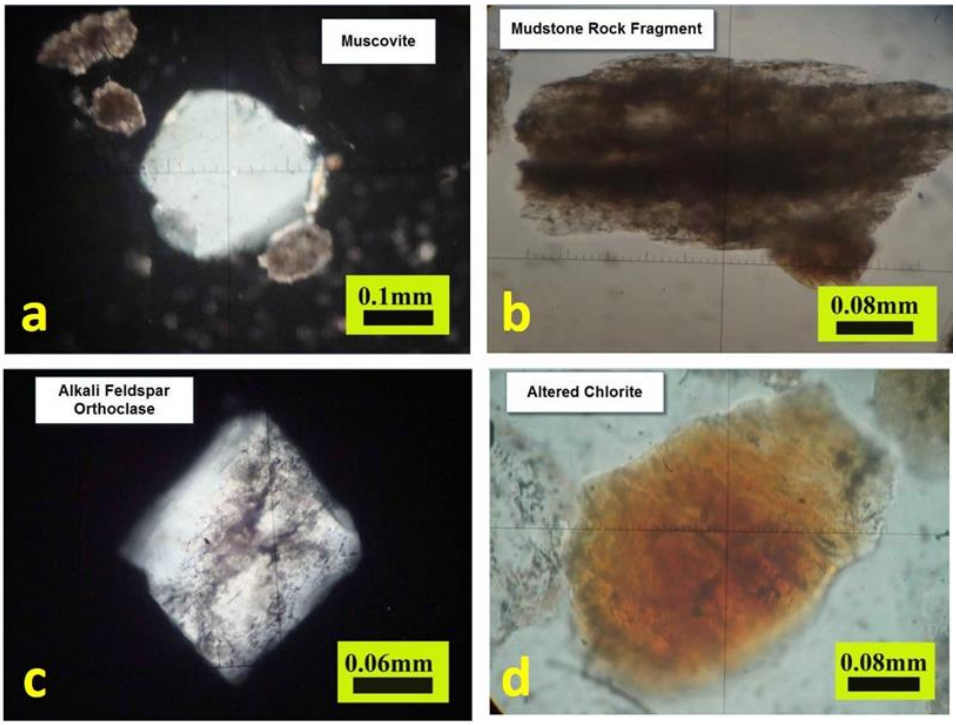

Fig. 8. Mineral composition of Pedon 2 surface horizon.

Figure 8 images showed muscovite as dioctahedral mica which appears with some effectiveness in weathering because muscovite is high resistance mineral beside mudstone rock fragments and alkali feldspar (orthoclase) with white color having some cracks by the effect of weathering, altered chlorite appears in yellow reddish color with weathered edges. Figure 9 shows opaque grains of iron oxides with black color and we can see the angular chert rock fragment coated by clay minerals (Fig. 9b), also high relief rounded colorless zircon which appears less effective as compared with zircon in Pedon 1 (Fig. 9c), secondary gypsum also appears as a cloud and in white color which may be formed in situ (Fig. 9d), this composition reflects the intensity of weathering which gave products in a mixed way.

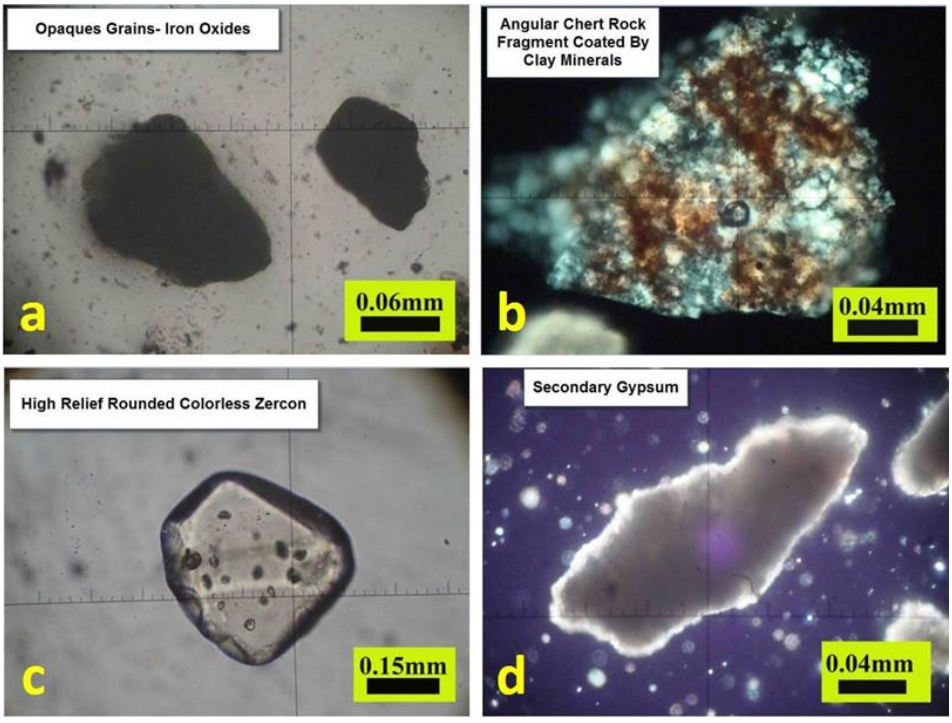

Fig. 9. Mineral composition of Pedon 3 surface horizon.

Figure (10) showed the mineral composition of Pedon 2 in the surface horizon where primary gypsum (yellowish color) appears which shows a difference with secondary gypsum that appears in Pedon 3 as a cloud with white color (Fig. 9d), also sub-rounded green color chlorite appears with some signs of weathering such as holes and broken edges, beside rounded altered deep green chlorite with spots of iron oxides which characterized by high pigmentation ability, this state also one from important features of weathering in this area, as add to the existence of altered light green amphibole which appears with irregularity on the surface fill of high and low zones and some holes with different sizes which occur as a result of weathering by reactions between water and these minerals in alkaline media which supported by some alkaline earth elements bearing minerals such as plagioclase feldspar.

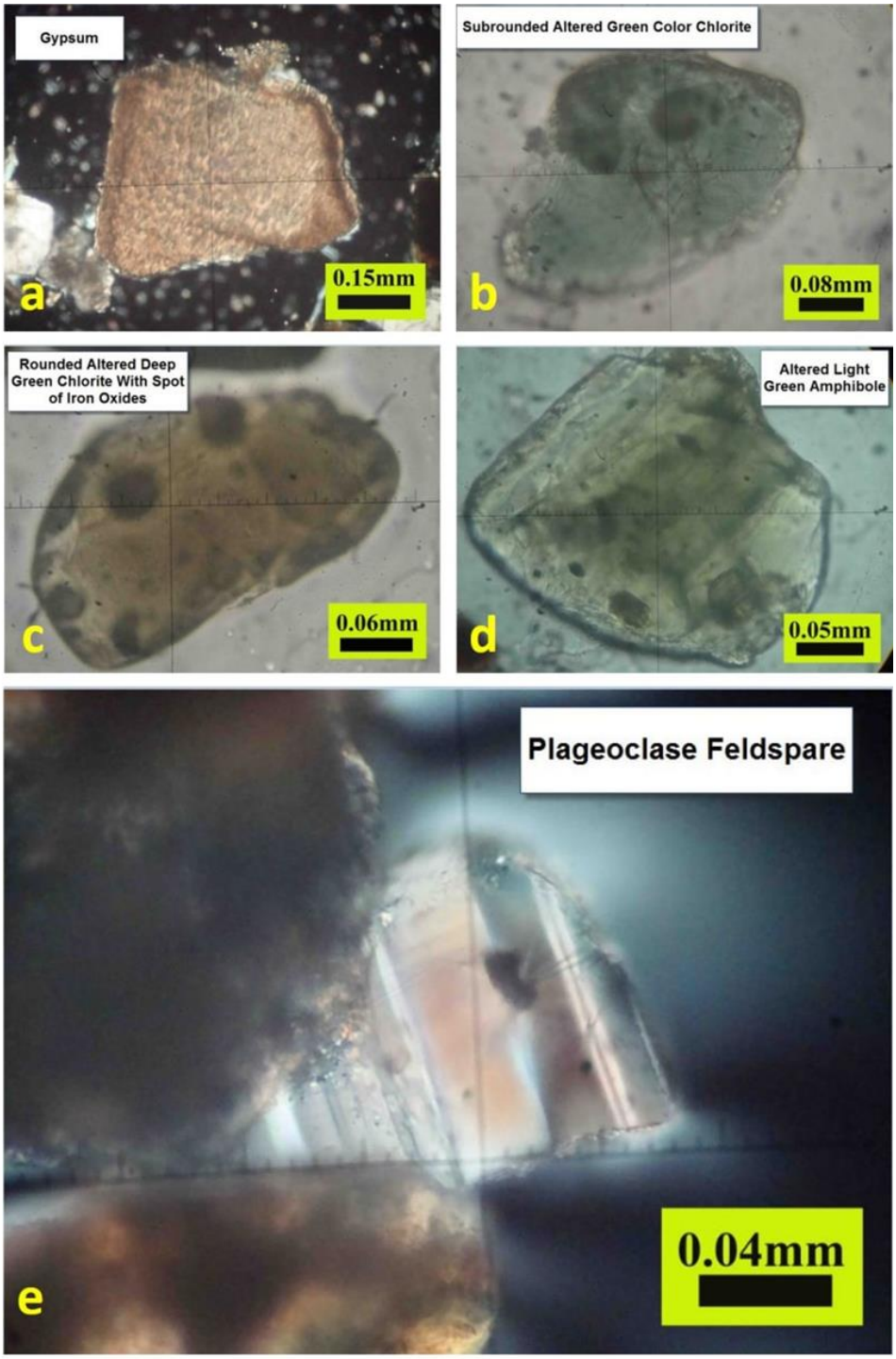

Fig. 10. Mineral composition of Pedon 2 surface horizon.

Conclusions

In alkaline conditions, because of mineral carbonate minerals richness, which characterizes by the low amount of precipitation. The intensity, and type of silicate minerals weathering are restricted not only by the climate but by the chemical conditions of the environment. Many weathering features are diagnosed in Al-Band Hills although it's located in semi-arid regions which supposed to be in low weathering intensity. This phenomenon could be explained by attributing these weathering features to the parent rocks source which transferred with river water and sediment in the area. Also, in an alkaline environment, many minerals can be a source of alkaline earth elements which cause rising in the pH of the soil solution and support the weathering intensity by increasing the ionic strength of the soil solution.

Acknowledgments

The authors would like to thank the Department of Geography at the University of Misan - Iraq and the Babylon Center for Civilization and Historical Studies University of Babylon - Iraq, for the scientific support they provided during the study period.

Conflict of Interest

The authors declare that there are no conflicts of interest regarding the publication of this manuscript.

References

Adamu, C.I., Oyetade, O.P., Ekwere, A.S., Kudamnya, E.A., Adebayo, K.I., Uyok, I.A., and Nganje, T.N., 2021. Mineralogical and Physico-Chemical Properties of the Cretaceous Shales of the Calabar Flank, South-Eastern, Nigeria: Implication for Paleo-Weathering Conditions, Provenance, and Industrial Applications. Solid Earth Sciences. https://doi.org/10.1016/j.sesci.2021.10.001.

Agha, O. M. A. M., and Şarlak, N., 2016. Spatial and Temporal Patterns of Climate Variables in Iraq. Arabian Journal of Geosciences, 9(4), 301–311. https://doi.org/10.1007/s12517-16-2324-y.

Baldermann, A., Dietzel, M., and Reinprecht, V., 2021. Chemical Weathering and Progressing Alteration as Possible Controlling Factors for Creeping Landslides. Science of the Total Environment, 778. https://doi.org/10.1016/j.scitotenv.2021.146300

Bickle, M.J., Chapman, H.J., Tipper, E., Galy, A., de La Rocha, C.L., and Ahmad, T., 2018. Chemical Weathering Outputs from the Flood Plain of the Ganga. Geochimica et Cosmochimica Acta, 225, 146–175. https://doi.org/10.1016/j.gca.2018.01.003.

Brosens, L., Robinet, J., Pelckmans, I., Ameijeiras-Mariño, Y., Govers, G., Opfergelt, S., Minella, J.P.G., and Vanderborght, J., 2021. Have Land Use and Land Cover Change Affected Soil Thickness and Weathering Degree in a Subtropical Region in Southern Brazil? Insights from Applied Mid-Infrared Spectroscopy. Catena, 207. https://doi.org/10.1016/j.catena.2021.105698.

Sparks, D.L., Page, A.L., Helmke, P.A., Loeppert, R.H., Soltanpour, P.N., Tabatabai, M.A., Johnston, C.T., Sumner, M.E., 1996. Methods of Soil Analysis Chemical Methods.

Delvigne, J., and Stoops, G., 1990. Morphology of Mineral Weathering and Neoformation. I. Weathering of most Common Silicates. Developments in Soil Science, 19(C), 471–481. https://doi.org/10.1016/S0166-2481(08)70362-3.

Dupré, B., Dessert, C., Oliva, P., Goddéris, Y., Viers, J., François, L., Millot, R., and Gaillardet, J., 2003. Rivers, Chemical Weathering and Earth's Climate. In Comptes Rendus – Geoscience, Vol. 335, Issue 16, pp. 1141–1160. Elsevier Masson SAS. https://doi.org/10.1016/j.crte.2003.09.015.

Dzombak, R.M., and Sheldon, N.D., 2022. Terrestrial Records of Weathering Indicate Three Billion Years of Dynamic Equilibrium. In Gondwana Research, Vol. 109, pp. 376–393. Elsevier Inc. https://doi.org/10.1016/j.gr.2022.05.009

Faksness, L.G., Altin, D., Størseth, T.R., Nordtug, T., and Hansen, B.H., 2020. Comparison of Artificially Weathered Macondo Oil with Field Samples and Evidence that Weathering does not Increase Environmental Acute Toxicity. Marine Environmental Research, 157. https://doi.org/10.1016/j.marenvres.2020.104928

Favier, S., Teitler, Y., Golfier, F., and Cathelineau, M., 2022. Multiscale Physical–Chemical Analysis of the Impact of Fracture Networks on Weathering: Application to nickel redistribution in the formation of Ni-laterite ores, New Caledonia. Ore Geology Reviews, 147, 104971. https://doi.org/10.1016/j.oregeorev.2022.104971

Graly, J.A., Licht, K.J., Bader, N.A., Kassab, C.M., Bish, D.L., and Kaplan, M.R., 2022. Chemical Weathering Signatures at Mt. Achernar, Central Transantarctic Mountains II: Surface exposed sediments. Geochimica et Cosmochimica Acta. https://doi.org/10.1016/j.gca.2022.06.024

Hartmann, J., and Moosdorf, N., 2011. Chemical Weathering Rates of Silicate-Dominated Lithological Classes and Associated Liberation Rates of Phosphorus on the Japanese Archipelago-Implications for global scale analysis. Chemical Geology, 287(3–4), 125–157. https://doi.org/10.1016/j.chemgeo.2010.12.004

Hartmann, J., Moosdorf, N., Lauerwald, R., Hinderer, M., and West, A.J., 2014. Global Chemical Weathering and Associated P-Release - the Role of Lithology, Temperature and Soil Properties. Chemical Geology, 363, 145–163. https://doi.org/10.1016/j.chemgeo.2013.10.025

Herrero, J., Ba, A.A., and Aragüés, R., 2003. Soil Salinity and its Distribution Determined by Soil Sampling and Electromagnetic Techniques. Soil Use and Management, 19(2), 119-126. https://doi.org/10.1111/J.1475-2743.2003.TB00291.X

Hussein, I.Q., 2014. The Effect of Climatic Water Budget on The Investment of Water Resources in the Governorate of Misan. Baghdad University.

Jackson, T.A., 2015. Weathering, Secondary Mineral Genesis, and Soil Formation Caused by Lichens and Mosses Growing on Granitic Gneiss in a Boreal Forest Environment. Geoderma, 251–252, 78–91. https://doi.org/10.1016/J.GEODERMA.2015.03.012

Jacob H.D. and Topp, G.C., 2002. Methods of Soil Analysis Part 4 Physical Methods.

Jassim, S.Z. and Goff, J.C., 2006. Geology of Iraq, Czech Repu. Dolin, Hlavni 2732.

Kalinin, P.I., Kudrevatykh, I.Y., Malyshev, V.V., Pilguy, L.S., Buhonov, A.V., Mitenko, G.V., and Alekseev, A.O., 2021. Chemical Weathering in Semi-Arid Soils of the Russian Plain. CATENA, 206, 105554. https://doi.org/10.1016/J.CATENA.2021.105554

Lybrand, R., Rasmussen, C., Jardine, A., Troch, P., and Chorover, J., 2011a. The Effects of Climate and Landscape Position on Chemical Denudation and Mineral Transformation in the Santa Catalina Mountain Critical Zone Observatory. Applied Geochemistry, 26(SUPPL.), S80–S84. https://doi.org/10.1016/J.APGEOCHEM.2011.03.036

Lybrand, R., Rasmussen, C., Jardine, A., Troch, P., and Chorover, J., 2011b. The Effects of Climate and Landscape Position on Chemical Denudation and Mineral Transformation

in the Santa Catalina Mountain Critical Zone Observatory. Applied Geochemistry, 26(SUPPL.), S80–S84. https://doi.org/10.1016/J.APGEOCHEM.2011.03.036

Maaroof, B.F., 2017. Geomorphological Characteristics of the East Tigris Region Between Al-Shihabi and Al-Huwaizah Marsh in Southeastern Iraq. Journal of Misan Researches, 13(26), 366–390.

Maaroof, B.F., 2022a. Geomorphological Assessment Using Geoinformatics Applications of the Sloping System of Al-Ashaali Drainage Basin at Iraqi Southern Desert. Iraqi National Journal of Earth Science, 22(1), 38–54. https://doi.org/10.33899/earth.2022.133146.1009

Maaroof, B.F., 2022b. Geomorphometric Assessment of the River Drainage Network at Al-Shakak Basin (Iraq). Journal of the Geographical Institute Jovan Cvijic SASA, 72(1), 1–13. https://doi.org/10.2298/IJGI2201001M

Maaroof, B.F., and Kareem, H.H., 2022. Geomorphometric Analysis of Al-Teeb River Meanders Between Al-Sharhani Basin and Al-Sanaf Marsh, Eastern of Misan Governorate, Iraq. In Misan Journal for Academic Studies, Vol. 42, Issue 21.

Al-Ghanmi, M.A., 2015. Hydrogeological Assessment Study of Al-Teeb Basin, East of Misan Governorate, p. 54. Ministry of Water Resources.

Mayer, L., and Mayer, L., 1986. The Distribution of Calcium Carbonate in Soils: A Computer Simulation Using Program CALSOIL. DOI: https://10.3133/ofr86155.

Millot, R., and Négrel, P., 2013. Chemical Weathering of Granitic Rocks: An Experimental Approach and Pb-Li Isotope Tracing. Procedia Earth and Planetary Science, 7, 590–593. https://doi.org/10.1016/j.proeps.2013.03.131

Mills, A.J., and Fey, M.V., 2013. Declining Soil Quality in South Africa: Effects of Land Use on Soil Organic Matter and Surface Crusting. https://doi.org/10.1080/02571862.2004.10635071

Négrel, P., Millot, R., Petelet-Giraud, E., Malcuit, E., and Brenot, A., 2013. Impact of Rock Weathering on the Chemical Composition of Groundwater Determined by Inverse Modeling in Large Sedimentary Basins. Procedia Earth and Planetary Science, 7, 615–619. https://doi.org/10.1016/j.proeps.2013.03.135

Nhu Sang, P., Liu, Z., Zhao, Y., Zhao, X., Dong Pha, P., van Long, H., and Van, H., 2018. Chemical Weathering in Central Vietnam from Clay Mineralogy and Major-Element Geochemistry of Sedimentary Rocks and River Sediments. Heliyon, 4, 710. https://doi.org/10.1016/j.heliyon.2018

Ojo, O.J., Adepoju, S.A., Awe, A., and Adeoye, M.O., 2021. Mineralogy and Geochemistry of the Sandstone Facies of Campanian Lokoja Formation in the Southern Bida Basin, Nigeria: Implications for Provenance and Weathering History. Heliyon, 7(12). https://doi.org/10.1016/j.heliyon.2021.e08564

Prajith, A., Tyagi, A., and Kurian, P.J., 2021. Geochemistry of Core Sediments from the Southeastern Bay of Bengal: Inferences on Weathering and Early Diagenetic Changes. Geoscience Frontiers, 12(2), 495–504. https://doi.org/10.1016/j.gsf.2020.08.011

Puttonen, T., Salmi, M., and Partanen, J., 2021. Mechanical Properties and Fracture Characterization of Additive Manufacturing Polyamide 12 After Accelerated Weathering. Polymer Testing, 104. https://doi.org/10.1016/j.polymertesting.2021.107376

Rozanov, A., Lessovaia, S., Louw, G., Polekhovsky, Y., and de Clercq, W., 2017. Soil Clay Mineralogy as a Key to Understanding Planation and Formation of Fluvial Terraces in the South African Lowveld. CATENA, 156, 375–382. https://doi.org/10.1016/J.CATENA.2017.04.027

Ruehlmann, J., 2020. Soil Particle Density as Affected by Soil Texture and Soil Organic Matter: 1. Partitioning of SOM in Conceptional Fractions and Derivation of a Variable SOC to SOM Conversion Factor. Geoderma, 375, 114542. https://doi.org/10.1016/J.GEODERMA.2020.114542

Saiz, G., Bird, M.I., Domingues, T., Schrodt, F., Schwarz, M., Feldpausch, T. R., Veenendaal, E., Djagbletey, G., Hien, F., Compaore, H., Diallo, A., and Lloyd, J., 2012. Variation in Soil Carbon Stocks and their Determinants Across a Precipitation Gradient in West Africa. Global Change Biology, 18(5), 1670–1683. https://doi.org/10.1111/J.1365-2486.2012.02657.X

Sissakian, V.K., and Fouad, S.F.A., 2015. Geological Map of Iraq, Scale 1: 1000 000. Iraqi Bulletin of Geology and Mining, 11(1), 9–17.

Ulery, A. L., and Drees, L. R., 2008. Methods of Soil Analysis. Part 5, Mineralogical Methods, APRIL L. ULERY and L. RICHARD DREES, Ed.; Soil Science. Soil Science Society of America, Inc., Madison, Wisconsin, USA.

Veras De Lima, H., Fabiola, N., Giarola, B., and Pires Da Silva, A., 2013. Porosity and Structure in Brazilian Hardsetting Soils: an Evaluation by 2D-Image Analysis. Revista de Ciências Agrárias Amazonian Journal of Agricultural and Environmental Sciences, 56(Suple), 107–114. https://doi.org/10.4322/rca.2013.089

Voigt, C., Klipsch, S., Herwartz, D., Chong, G., and Staubwasser, M., 2020. The Spatial Distribution of Soluble Salts in the Surface Soil of the Atacama Desert and their Relationship to Hyperaridity. Global and Planetary Change, 184, 103077. https://doi.org/10.1016/J.GLOPLACHA.2019.103077

Walk, J., Bartz, M., Stauch, G., Binnie, A., Brückner, H., and Lehmkuhl, F., 2022. Weathering under coastal hyperaridity – Late Quaternary Development of Spectral, Textural, and Gravelometric Alluvial Fan Surface Characteristics. Quaternary Science Reviews, 277. https://doi.org/10.1016/j.quascirev.2021.107339

Wilford, J., 2012. A Weathering Intensity Index for the Australian Continent Using Airborne Gamma-Ray Spectrometry and Digital Terrain Analysis. Geoderma, 183–184, 124–142. https://doi.org/10.1016/J.GEODERMA.2010.12.022

Yousefifard, M., Ayoubi, S., Poch, R. M., Jalalian, A., Khademi, H., and Khormali, F., 2015. Clay Transformation and Pedogenic Calcite Formation on a Lithosequence of Igneous Rocks in Northwestern Iran. CATENA, 133, 186–197. https://doi.org/10.1016/J.CATENA.2015.05.014

Yusoff, I.N., Mohamad I.M.A., Tobe, H., Date, K., and Yokota, Y., 2022. Quantitative Granitic Weathering Assessment for Rock Mass Classification Optimization of Tunnel Face Using Image Analysis Technique. Ain Shams Engineering Journal. https://doi.org/10.1016/j.asej.2022.101814